Iterative time reversal based crack identification

Robert Seidl*[1] and Ernst Rank[1,2]

[1]Chair for Computation in Engineering, Technische Universität München, Arcisstr. 21, 80333 München, Germany
[2]Institute for Advanced Study, Technische Universität München, Germany

Abstract

In the field of ultrasonic non destructive testing ultrasonic impulses are used to detect cracks in components without causing damage. When performing only experiments it is possible to infer the state of the component but usually no additional details about the interior damage like position, dimension or orientation are available. Furthermore, the amount of sensors that can be used to record the signals is limited to only a few because of the shape and dimension of typical specimen. The information about these details is hidden in the recorded experimental signals. The idea of the proposed method is to use this experimental data together with a wave speed model of the healthy component and to try to adapt the model to generate these experimental measurements. Formally, the problem is posed as nonlinear optimization and the wave speed model is adapted such that the discrepancy between experimental measurements and the model output is minimized. Moreover, to overcome the problem of only few available sensor measurements, a combination of multiple experiments is used to improve accuracy. Following this approach, the position, dimension and orientation of a crack is detected for an emulated cracked aluminum plate. When only few sensors are available, it is shown how a combination of similar experiments can be used to improve the inversion results.

Keywords: Full waveform inversion, iterative adjoint-based optimization, crack detection, ultrasonic non destructive testing, adjoint method, time reversal, finite differences

1 Introduction

The goal of structural health monitoring (SHM) is the implementation of a damage detection and characterization strategy for physical structures. In this context, a damage is defined as a change in either material or geometric properties of the structural system. SHM is concerned with the observation of a state of such a system over time using response measurements from an array of sensors and its goal is the extraction of damage-sensitive features from these measurements. Principal techniques consist of vibration based and wave propagation based techniques. Methods in nondestructive testing (NDT) use electromagnetic, radiation, sound and inherent properties of materials to examine samples. Application areas are weld verification, radiography in medicine or structural mechanics. In the latter, a structure undergoes a dynamic input such as a tap of a hammer or a controlled pulse and displacement or acceleration is measured at different sensor locations. Then, the observed output is compared to the expected output of the healthy structure. Thus, differences in outputs may indicate an inappropriate model or failed components. Possible methods include radiological, electrical, magnetical, and ultrasonic methods. Typical are x-ray tomography, eddy current or ultrasonic testing. The most widely used testing method is ultrasonic NDT. It is based on the propagation of low

*robert.seidl@tum.de, Corresponding Author

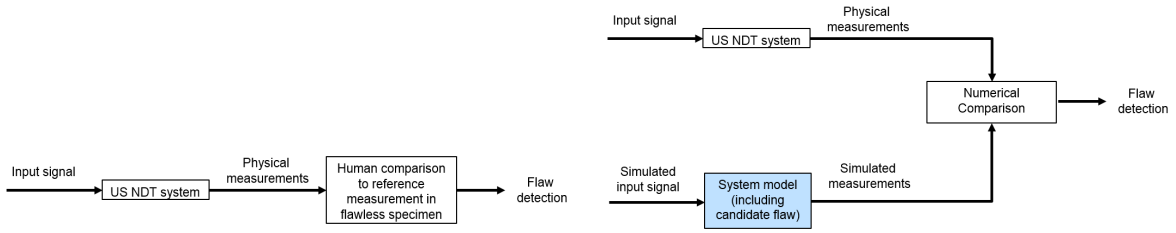

(a) expert based **(b)** flaw model based

Figure 1. Different NDT devices, after Amitt et al. [2014]

amplitude waves through material and measures the traveltime and intensity of the waves at certain sensors. In general, only radiological and ultrasonic techniques can detect internal flaws accurately. For an introduction into ultrasonic NDT see, e.g., Drinkwater and Wilcox [2006], Blitz and Simpson [1996] or Chakroun et al. [1992]. Ultrasonic NDT is extensively employed in the aircraft, nuclear, oil and gas industries. Very short ultrasonic pulse waves with center frequencies ranging from 0.1 - 20 MHz and wavelengths in the range of 1 to 10 mm are transmitted into materials to detect internal flaws. Advantages of ultrasonic NDT are that it allows to detect flaws deep in the part, permits the detection of extremely small flaws (in order of the wavelength of the source) and has some capabilities of estimating the size, orientation and shape of defects. In principle, cracks and other discontinuities being hidden in the structure produce reflective interfaces and can be detected using ultrasonic NDT.

Classical ultrasonic NDT methods were parameter-based, because it was not possible to store the entire signal at every sensor for earlier devices. The idea is to assume that the measured signals can be described sufficiently accurate by a set of parameters. Examples for such parameters are the maximum peak-to-peak amplitude, arrival time, rise time or duration of the signal, see Grosse [2008] for a general overview. In the classical approach the physical measurements, or some selected features of them, are compared to reference measurements in the flawless specimen by a human expert who then decides if there is a flaw in the specimen or not based on hand-made criteria. This standard NDT device has the capability to detect damage but usually not to provide detailed information on the damage parameters. The principle setup for a purely experimental NDT device is shown in Fig.1a.

More recently it has been possible to store the complete signals allowing to couple experimental data with numerical simulation models. Recently, Amitt et al. [2014] introduced an approach that is based on a combination of the experimental measurements and a simulation model. Fig. 1b shows this model-based NDT system where a flaw is identified based on a comparison to a computational model which assumes various candidate flaws. The position of these is varied to find the best fit. The key idea of this approach is to use the concept of time reversal, see Fink [1997]. It is based on the reversibility property of wave propagation, letting developed signals propagate back in time to the location of the source that emitted them originally. If the source is very local this procedure is called refocusing. It can be divided into three parts. First, a known source generates waves in the structure and the time-varying response of the structure is measured at certain points and times. Second, using a computational model of the structure, the measured signals are played back into the structure to construct a time reversal solution for each set of crack parameters. A specific measure is used to find the initialization time at the original source. Third, the crack identification problem is posed as optimization problem: "*Among all crack candidates, find the crack which yields the best wave refocusing at the true source location.*" See Amitt et al. [2014] and Givoli and Turkel [2012] for more details.

Time reversal methods have been used extensively in seismology, see Larmat et al. [2010],Farova and Krus [2012],Fink [1997],Fink et al. [2000],Kremers et al. [2011], Tromp et al. [2008]. Recently, this approach has been extended to the so called full waveform inversion, which is used to create

high-resolution wave speed models. It performs forward modeling to compute the differences between the acquired seismic data and the current model as well as a process similar to reverse-time migration (RTM) of the residual dataset to compute a gradient and to update the wave speed model. See Fichtner [2011] for more details. As the parameter space for these wave speed models is often extremely high dimensional (one parameter may be assumed for one finite element in a 3D finite element model) the method relies on adjoint-based techniques to compute the gradient efficiently. Similar methods have been used in many other fields of applications, where high dimensional parameter spaces need to be treated. Among these are computational fluid dynamics, Giles and Pierce [2000],Giles and Pierce [1997], aerodynamics, Jameson [1988], Gauger [2002] and shape optimization Newman III et al. [1999],Bletzinger and Ramm [2014]. Most recently the method has been applied for elastic media in Fathi et al. [2015]. We prefer to call the method iterative time-reversal based optimization to emphasize that in the case of wave propagation time-reversal can be regarded as one of the key building blocks of this algorithm. We show the applicability and benefits of this method in the field of ultrasound NDT.

The paper is organized as follows. Section 2 introduces the concept of our method. Then the theoretical background of the gradient-based optimization procedure being able to identify a crack is presented in section 3. Section 4 shows numerical results for a model emulating a two-dimensional cracked aluminum plate. Furthermore, we study how the quality of the detection of dimension and position of the crack is affected by different locations of the ultrasonic source, the crack location and the placement of the sensors respectively. We investigate how a typically small amount of sensors can be used for damage detection by combining outcomes of multiple experiments in a slightly modified cost function. Section 5 summarizes the results and gives an outlook of possible research directions.

2 Concept of an iterative adjoint-based system identification

One limitation of the proposed method of Amitt et al. [2014] is the need of prior knowledge of both crack dimension and orientation. Instead of relying on candidate flaws, we try to solve the problem in a more general way based on the concept of iterative adjoint-based optimization. For some general literature see Marchuk [1995] or Lions [1971]. The typical setup in an ultrasonic (US) NDT experiment is the following. An ultrasonic source is applied somewhere on the structure, like a block of concrete or a metal plate, and the response is measured by a rather small number of sensors that are connected to the structure. The starting point of the method is the sole knowledge of this sensor signals from the experiment. Furthermore, knowledge of the details of the experiment is assumed. For example, what source signal was used and where the ultrasonic source was applied. The structure under testing is possibly cracked and it is assumed that a suitable numerical model of the corresponding healthy structure is available. The acoustic wave equation is used to model the propagation of compression waves in the medium with a spacial variable wave speed $v_p(x)$.

$$u_{tt}(x,t) - v_p^2(x)\Delta u(x,t) = f_s(x,t) \text{ for } x \in \Omega \subset \mathrm{R}^2 \text{ or } \mathrm{R}^3,\ t \in [0,T] \tag{1a}$$

$$u(x,0) = u_t(x,0) = 0, \text{ on } \Omega \tag{1b}$$

$$u = 0 \text{ on } \partial\Omega \tag{1c}$$

Equation 1 describes the structural displacement field u induced by an applied ultrasonic impulse f_s in a two- or three-dimensional domain Ω for a time span of T (micro) seconds, modeled by the acoustic wave equation. All boundaries are assumed to be fully reflective. Here, v_p is the speed of pressure waves in the material. The impulse f_s is modeled as a point source, $f_s = A(t) \cdot \delta(x - x_s)$, where x_s is the source position and $A(t)$ is the time-varying amplitude of the source. Importantly, the p-wave speed v_p of the acoustic simulation model is assumed to be piecewise constant on a fine

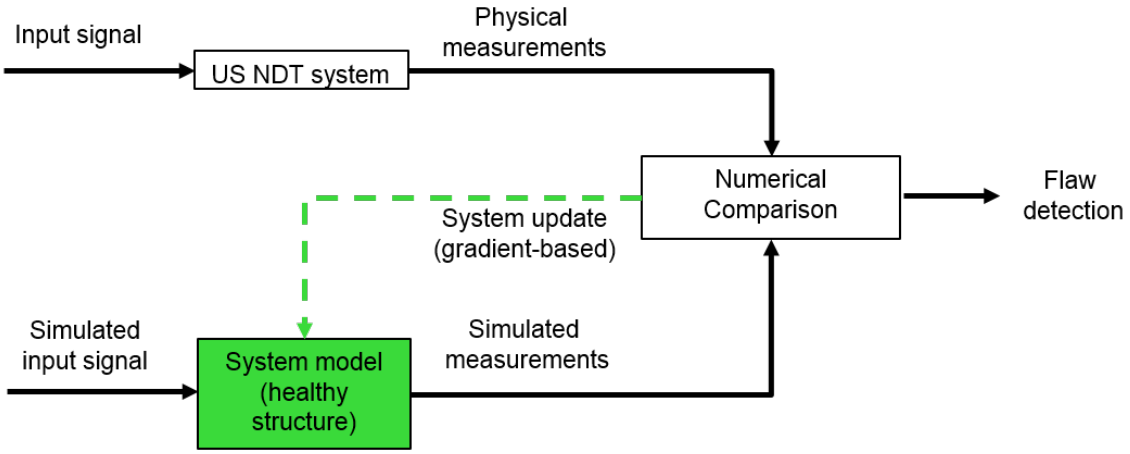

Figure 2. Adaptive model-based NDT device

enough predefined grid being able to represent the crack. The solution is measured at n distinct sensor locations $x_i^r, i = 1, \ldots, n$.

Without any further prior knowledge, this model is used together with the experimental setting to generate comparable signals at virtual sensors. If the experimental structure is cracked these synthetic measurements $u(x_r, t)$ and the physical measurements $u_0(x_r, t)$ differ at all sensor locations x_r. The idea is to try to minimize this difference (over all sensors and time steps) by adapting the underlying wave speeds v_p of the simulation. How this inverse problem is formulated as optimization problem is discussed in the next section.

In contrast to Amitt et al. [2014] it is not tried to reconstruct the correct position of the known source but instead it is tried to infer the location where the presence of the crack led to a scattering of the waves. To do this, a three-step procedure is used. First, the numerical simulation of the healthy structure generates measurements which can be compared to the observed data. Taking now the difference of both signals (over all sensor locations) cancels the parts of the signals that are related to the primary waves stemming from the ultrasonic source. What remains are only the recorded waves that originate from the scattering at the crack. Second, the concept of time reversal is used for these difference signals; they are time reversed for them and all former sensors act as sources in a second simulation. This results in a focusing at the crack location. Third, a combination of this time reversal solution and the forward simulation is used to identify regions in the structure that are responsible for the crack.
The objective can be formulated verbally: *Adapt the propagation speed v_p of the model such that the simulated signals are as close as possible to the observed signals from the experiment.*
Formulating this PDE constrained nonlinear minimization problem, a suitable optimization method has to be chosen. For this a simple gradient-based minimization procedure is used which is the topic of the next section.

When formulating the problem this way, it does not rely on prior knowledge of dimension and location of candidate flaws. The concept can be interpreted as an adaptive model-based NDT device. This is depicted in Figure 2. The system model is given by a simulation model of the healthy structure and its speed field is adapted by a gradient-based minimization process that tries to reconstruct the observed measurements. Given enough sensor measurements, the adapted model is able to provide information on the size, orientation and shape of the crack in the interior.

3 Theoretical Background

For later use, the differential operator L as $L(u,m) := u_{tt} - m\Delta u$ is defined, where u fulfills the initial and boundary conditions and one uses $L(u,m) = f_s$ for a short hand of equation (1). In principle, any numerical method being suitable for its solution like finite elements or finite differences can be used. In the numerical studies a simple finite difference scheme is applied using the same computational grid as the one which is taken for defining the piecewise constant p-wave speed v_p. The solution of the forward problem generates sensor signals that are expected to be measured, when the healthy structure is tested. If the structure is cracked, then there will be a discrepancy between expected and measured signals because of a scattering of the ultrasonic pulse at the crack. Formally, the misfit is defined to be the cumulative least squares error between measured and expected signals at the sensor locations $x_i^r, i = 1, \ldots, n$ over the time period $[0, T]$.

$$\chi(m) = \frac{1}{2} \sum_{i=1}^{N} \int_0^T \int_\Omega [u(m;x,t) - u^0(x,t)]^2 \delta(x - x_i^r) \, \mathrm{d}t \, \mathrm{d}x \tag{2}$$

Here, the experimental measurements are given by $u^0(x,t)$ and $u(m;x,t)$ is the solution of the acoustic wave equation for a given material model $m(x) := v_p(x)^2$. The question to be answered is a calibration problem: *How do we need to change the wave speeds to generate signals at the sensors that are similar to the ones observed from the experiment?*
The goal is to try to minimize the misfit $\chi(m)$ by adapting $m(x)$ in the simulation model.
This inverse problem can, in principle, be tackled using non-linear optimization methods. For a comprehensive overview on theory and methods see e.g. Nocedal and Wright [1999], Fletcher [2008], Polak [1997] and Quarteroni et al. [2000]. As inverse problems are per definition ill-posed, it is not expected to be able to reconstruct the true crack exactly but the hope is that even a local minimum of the misfit is able to give insight about the position and dimension of the crack in the structure under testing.

Mathematical formulation

The misfit $\chi(m)$ is minimized by iteratively constructing a sequence of models $\{m_i\}_{i=1}^n$ that gradually decreases $\chi(m)$. A gradient descent method is used for this purpose. This is beneficial because, as will be shown, the gradient of the misfit with respect to model parameters m can be computed very efficiently using the adjoint state method.

Gradient descent

Given the actual model m_i the model is improved by employing the following update.

$$m_{i+1} = m_i + \gamma_i h_i \tag{3}$$

Here, h_i is a descent direction of χ and γ_i is a step size that fulfills $\chi(m_{i+1}) < \chi(m_i)$. In the case of steepest descent, the negative gradient is chosen as suitable direction.

$$h_i = -\nabla_m \chi(m) \tag{4}$$

Efficient adjoint-based gradient computation

Due to the very large number of model parameters a finite difference based gradient computation is not feasible. The adjoint state method avoids the computation of the sensitivity of the forward wave field to variations in the p-wave speeds by a clever construction of an adjoint state that can

be interpreted as the solution of the same acoustic wave equation for a different source function. General introductions to adjoint methods can be found in Marchuk [1995], Gauger [2002] and Errico [1997]. We closely follow Fichtner [2011] for the mathematical derivation. To simplify we start by rewriting the misfit as a general functional $\chi_1(m)$ that is integrated in space and time.

$$\chi(m) = \int_T \int_\Omega \chi_1[u(m;x,t)]\,\mathrm{d}t\,\mathrm{d}x = \langle \chi_1(m) \rangle \tag{5}$$

In our specific case, $\chi_1(m) := \frac{1}{2}\sum_{i=1}^{N}[u(m;x,t) - u^0(x,t)]^2\delta(x - x_i^r)$. The derivative $\nabla_m\chi\,\delta m$ of $\chi[u(m)]$ with respect to m in direction δm follows from the chain rule:

$$\nabla_m\chi\,\delta m = \nabla_u\chi\,\delta u = \langle \nabla_u\chi_1\,\delta u \rangle$$

where $\delta u := \nabla_m u\,\delta m$ denotes the derivative of u with respect to m in direction δm and $\langle . \rangle$ is a short notation for the double integral over $\Omega \times I$. The appearance of δu poses a problem. If we want to use finite differences to approximate this sensitivity then we need to evaluate $u(m + \epsilon\delta m)$ for a large number of directions δm. This is clearly infeasible for large model spaces because each evaluation corresponds to a solution of the acoustic wave equation. Therefore, the goal is to avoid the calculation of δm completely.
To accomplish this, start by deriving the acoustic wave equation using the chain rule to get the forward sensitivity PDE.

$$\nabla_m L\,\delta m + \nabla_u L\,\delta u = 0 \tag{6}$$

As next step introduce an arbitrary test function $u^\dagger$, multiply it with the state equation and integrate over space and time.

$$\langle u^\dagger \cdot \nabla_m L\,\delta m \rangle + \langle u^\dagger \cdot \nabla_u L\,\delta u \rangle = 0 \tag{7}$$

As this equation still evaluates to zero, add it to the misfit with the goal to eliminate δu.

$$\nabla_m\chi\,\delta m = \langle \nabla_u\chi_1\,\delta u \rangle + \langle u^\dagger \cdot \nabla_u L\,\delta u \rangle + \langle u^\dagger \cdot \nabla_m L\,\delta m \rangle \tag{8}$$

Rewrite (8) using the adjoint operators $\nabla_u\chi_1^\dagger$ and $\nabla_u L^\dagger u^\dagger$. They are defined as follows:

$$\langle \nabla_u\chi_1\,\delta u \rangle = \langle \delta\, u \cdot \nabla_u\chi_1^\dagger \rangle \tag{9}$$

and

$$\langle u^\dagger \cdot \nabla_u L\,\delta u \rangle = \langle \delta\, u \cdot \nabla_u L^\dagger u^\dagger \rangle \tag{10}$$

In our case boundary conditions of primal and adjoint operators coincide but initial conditions in the primal problem result in terminal conditions in the adjoint problem. These are due to the partial integration that needs to be done in order to construct the adjoint operator. Then we obtain

$$\nabla_m\chi\,\delta m = \langle \delta\, u \cdot (\nabla_u\chi_1 + \nabla_u L^\dagger u^\dagger) \rangle + \langle u^\dagger \cdot \nabla_m L\,\delta m \rangle \tag{11}$$

Now, if we can find a field $u^\dagger$ that satisfies the adjoint equation

$$\nabla_u L^\dagger u^\dagger = -\nabla_u\chi_1^\dagger \tag{12}$$

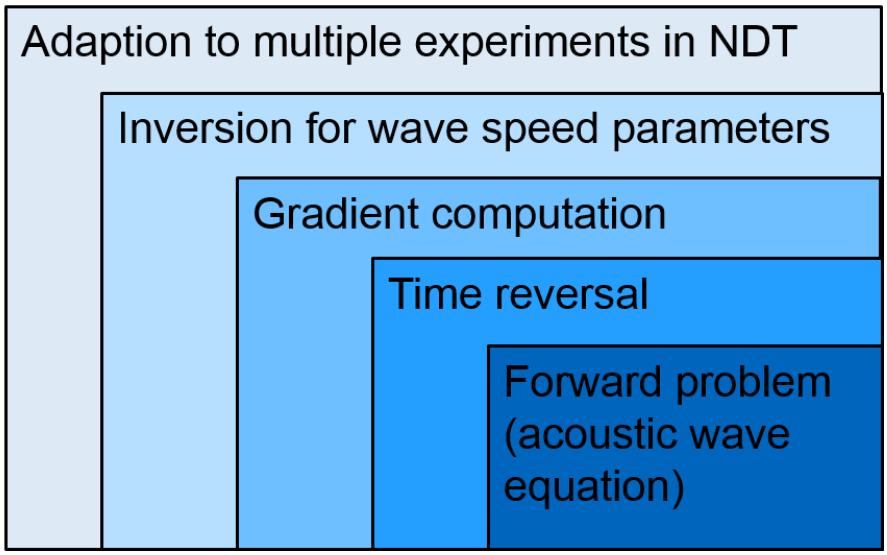

Figure 3. Conceptional overview of inversion algorithm.

we can completely avoid the calculation of δu and the gradient $\nabla_m \chi \, \delta m$ is given by

$$\nabla_m \chi \, \delta m = \langle u^\dagger \cdot \nabla_m L \, \delta m \rangle. \tag{13}$$

This way, the computation of the sensitivities of u is shifted to the computation of two adjoint operators $\nabla_u \chi_1^\dagger$ and $\nabla_u L^\dagger u^\dagger$ and one solution to the adjoint equation. Now, $\nabla_m \chi \, \delta m$ can be computed without the explicit knowledge of δu.
In our case the adjoint solution $u^\dagger$ needed for the gradient computation is the solution of the following PDE.

$$u_{tt}^\dagger(x,t) - v_p^2(x) \Delta u^\dagger(x,t) = f_s^\dagger(x,t) \text{ for } x \in \Omega \subset \mathrm{R}^2 \text{ or } \mathrm{R}^3, \; t \in [0,T] \tag{14a}$$

$$u^\dagger(x,T) = u_t^\dagger(x,T) = 0, \text{ on } \Omega \tag{14b}$$

$$u^\dagger = 0 \text{ on } \partial\Omega \tag{14c}$$

where

$$f_s^\dagger(x,t) := \sum_{i=1}^{N} [u(m;x,t) - u^0(x,t)] \delta(x - x_i^r).$$

Equation (14) refers to the adjoint problem. Spatial boundary conditions carry over one to one but temporal conditions change from initial conditions to terminal conditions. The adjoint source is built as superposition of sources that act at single points, the sensor positions, and its time function consists of the residual between observed and synthetic data. Because of the somewhat unusual terminal conditions, solving the adjoint equations can be interpreted as a propagation of residuals backwards in time from T to 0. Finally, the gradient can be obtained by calculating the quantity

$$\nabla_m \chi \, \delta m = \int_\Omega \int_0^T \Delta u \cdot u^\dagger \, dt \, dx. \tag{15}$$

After computing the gradient the second part of the algorithm consists of finding a step length γ_i. In the current implementation, the simplest approach of testing different step lengths and choosing

the one that decreases the misfit by the largest amount. Using other strategies like backtracking line search would improve the efficiency of the algorithm. The minimization process is terminated after a fixed number of iterations. The concept of the algorithm is summarized in Figure 3.

4 Numerical examples

In this section the proposed inversion method is applied to detect a crack in a simulated aluminum plate. Both, the plate and the crack are idealized in the following ways. The plate is assumed to be a two dimensional rectangular domain of dimension 100 mm x 200 mm. All boundaries are considered fully reflective. Therefore, no loss of acoustic energy is assumed. An ultrasonic point source is applied on the plate to scan the specimen. It is modeled as Ricker wavelet pulse with dominant frequency $f_0 = 200\,kHz$:

$$f_s(x,t) = f_0^2 \cdot (t - t_0) \cdot \exp(-f_0^2 \cdot (t - t_0)^2) \cdot \delta(x - x_0) \tag{16}$$

where t_0 is the delay and x_0 the position where the point source is applied. The propagation of pressure waves is modeled by the acoustic wave equation. Experimental sensor data is emulated using a second simulation model. In it, a crack is modeled as a small region where the wave speed model deviates from the background wave speed of aluminum of $v_p = 6420\frac{m}{s}$ by $v_c = 4600\frac{m}{s}$. Moreover, 2 % Gaussian noise is added to the sensor data to emulate measurement errors. The wave propagation of the pulse is modeled for a time span $\Delta T = 48\,\mu s$.

Finite differences in space and time, with accuracy of $O(\Delta x^4)$ and $O(\Delta t^2)$, are used for the numerical solution of the underlying forward and adjoint wave propagation problems 1 and 14. (see LeVeque [2007]).

$$\frac{\partial^2 u_{i,j}}{\partial^2 x} \approx \frac{-u_{i-2,j} + 16u_{i-1,j} - 30u_{i,j} + 16u_{i+1,j} - u_{i+2,j}}{12\Delta x^2} + O(\Delta x^4) \tag{17}$$

$$\frac{\partial^2 u_{i,j}}{\partial^2 y} \approx \frac{-u_{i,j-2} + 16u_{i,j-1} - 30u_{i,j} + 16u_{i,j+1} - u_{i,j+2}}{12\Delta y^2} + O(\Delta y^4) \tag{18}$$

$$u_{i,j}^{(t+1)} \approx 2u_{i,j}^{(t)} - u_{i,j}^{(t-1)} + \alpha_{i,j}(\frac{\partial^2 u_{i,j}}{\partial^2 x} + \frac{\partial^2 u_{i,j}}{\partial^2 y}) \cdot \Delta t^2 + O(\Delta t^2) \tag{19}$$

The spatial discretization of the plate is one gridpoint per mm^2. It is chosen fine enough to be able to resolve different crack positions. The simulation time is discretized by 1000 timesteps. This fine temporal resolution is used to generate a smooth source signal. The simulation time span is chosen such that the wavefront moves at least once through the complete domain. The discretization results in 20000 parameters for the adaptable wave speed.

General case

In a first computation the numerical experiment restricts to one fixed source position and searches for unknown cracks with different orientation relative to the source. One sensor at every grid point is used to simulate perfect knowledge of the complete numerical wave field.

Figure 4 shows four test cases only differing by the crack orientation. The position of the source is depicted by a black circle.

The minimization algorithm is stopped after 40 iterations, when in all cases a (local) minimum was reached. Figure 5 shows an example of the achieved decrease for different test cases.

The resulting wave speeds after the inversion are shown in Figure 6. The deviation of the final wave speed model from the initial homogeneous model is depicted. The left column visualizes the results

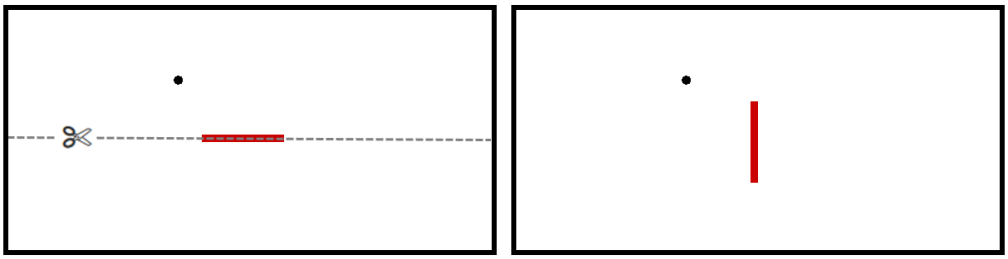

(a) Horizontal crack **(b)** Vertical crack

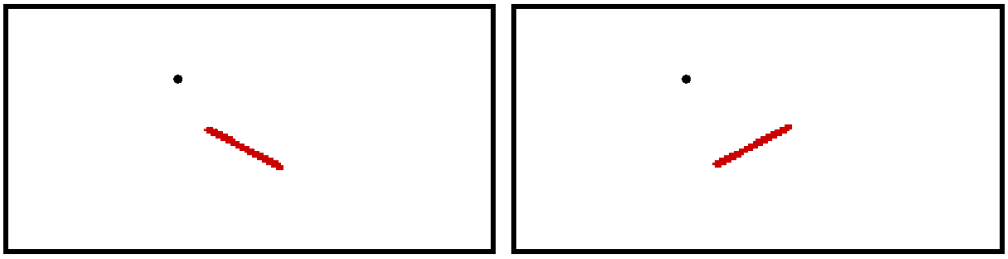

(c) Crack turned away from source **(d)** Crack facing source

Figure 4. The different test cases for the crack detection algorithm. The US source is depicted by a black circle. The crack is shown in red.

when the knowledge of the full wavefield is assumed for the misfit. The crack, its position, dimension and orientation is clearly visible. Due to the simultaneous update of all wave speed parameters in every iteration, some artificial noise is introduced in regions where the wave speed of the true model did not change.

In many practical cases - in particular in NDT for solid structures - it is not possible to place sensors in the interior of a body. Therefore, the following investigations restrict sensor positions to the boundary of the structure. In these experiments only partial information of the wavefield is captured by the misfit where only one sensor is placed at every grid point on the *boundary of the domain* leading to 600 sensors in total. The results are depicted in the right column of Figure 6. Black boxes on boundary layers indicate that the complete boundary was equipped with sensors. Clearly, crack position, dimension and orientation are still visible.

A horizontal cut through the wave speed model at the level of the crack as indicated in 4a allows to compare the quality of the inversions. Figure 7 shows the resulting wave speed. The crack is clearly visible in all test cases, even though the inversion did not lead to a perfect inference of the unknown wave speed parameters. The restriction to sensors on the boundary lead to a slightly worse result.

Furthermore, the results indicate that the accuracy of the inversion depends not only on the number and positioning of the sensors but also on the source location, as both inversions are better in identifying the closer edge of the crack.

To verify this, in the next computation, the same ultrasonic pulse is applied but its position is varied from position A over B to C. Results for the full wavefield case as shown on the right in Figure 7.

Comparing the results of varying the source position with the true wave speed model, the following details are observed, as shown in Figure 7a. First, the quality of the inversion results clearly depends on the positioning of the source relative to the unknown crack location. In position A, the US pulse

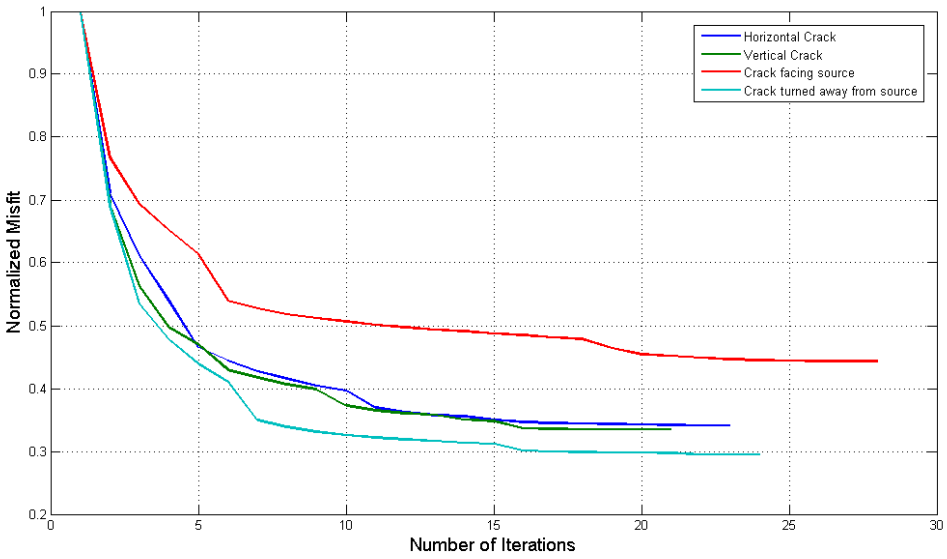

Figure 5. Evolution of misfit functional

is more accurate in identifying the left part of the crack. When the source is positioned in a way where there are strong reflections of the waves from the complete crack, as it is the case when placing the source at position B, the inversion is better able to grasp the homogeneity and dimension of the crack. If the source is positioned further to the right, only the right vertex of the crack is found to give the almost correct wave speed model. Therefore source position is crucial for the inversion success. This is a major drawback that is addressed later.

Reducing the number of sensors

Up to now, it was assumed that complete information on the whole wavefield or part of it on the boundary is available. This assumption of one sensor per grid point resulted in an unrealistic large number of sensors. Further investigations are restricted to the horizontal crack in test case A. As it is realistic to assume that sensors can only be positioned on the boundary surface in 3D, the focus is on a similar setup in the 2D plate problem. The next study investigates how the quality of the inversion changes, when the number of sensors is reduced to a more realistic amount.

In a first computation 16 sensors are put on the boundary as shown on the right in 8a. In a second computation only ten sensors are used which are depicted by green diamonds and both red sensors on the top and bottom. A third experiment only uses the four red sensors. Figure 8a shows the resulting wave speed field cutting through the horizontal crack and the corresponding setup on the right. The position, orientation and dimension of the crack is still visible for all experiments. But decreasing the number of sensors clearly decreases the inversion quality. On a first glance, these are rather unpromising results for realistic cases. The key here is to recognize that the more information is available in the misfit the better the inversion results will be. We focus on this topic in the next section.

Combining experiments

Previously, it was shown that the quality of the inversion heavily depends on the position of the source with respect to the crack location. Because the crack position is not known a priori a possible

Figure 6. Inversion results for all test cases assuming one sensor per grid point (left column) or one sensor per grid point on the boundary (right column). Black rectangles indicate that only boundary measurements where used.

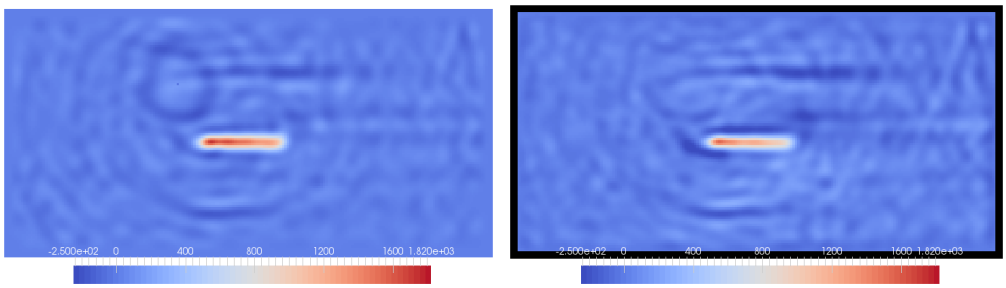

(a) Horizontal crack **(b)** Horizontal crack

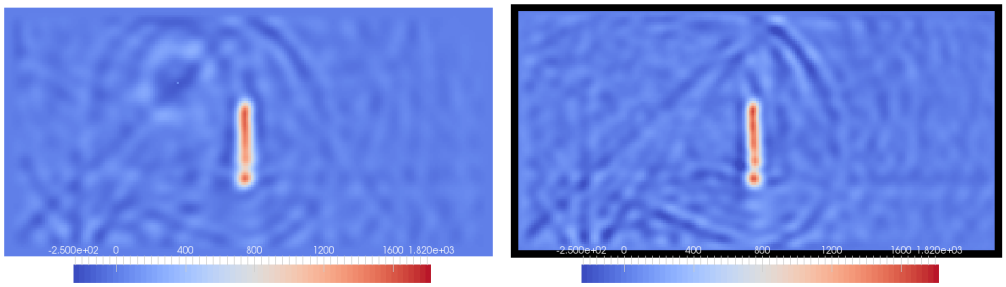

(c) Vertical crack **(d)** Vertical crack

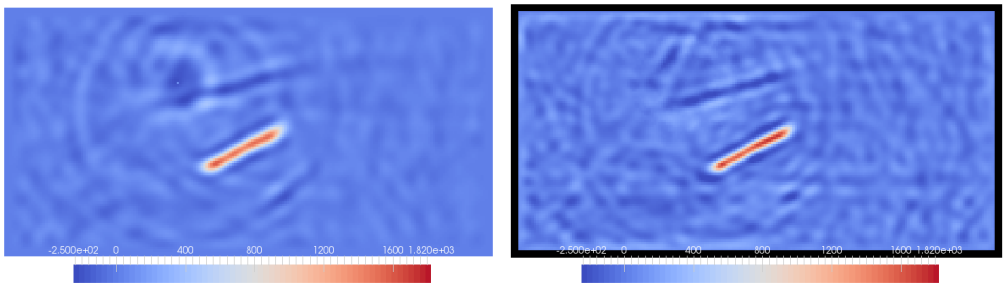

(e) Crack facing source **(f)** Crack facing source

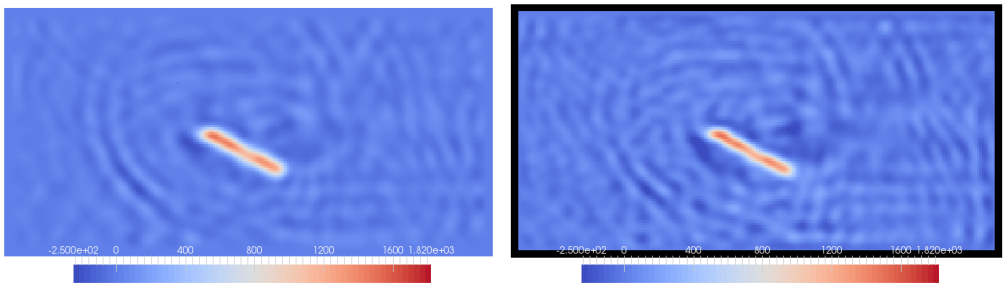

(g) Crack turned away from source **(h)** Crack turned away from source

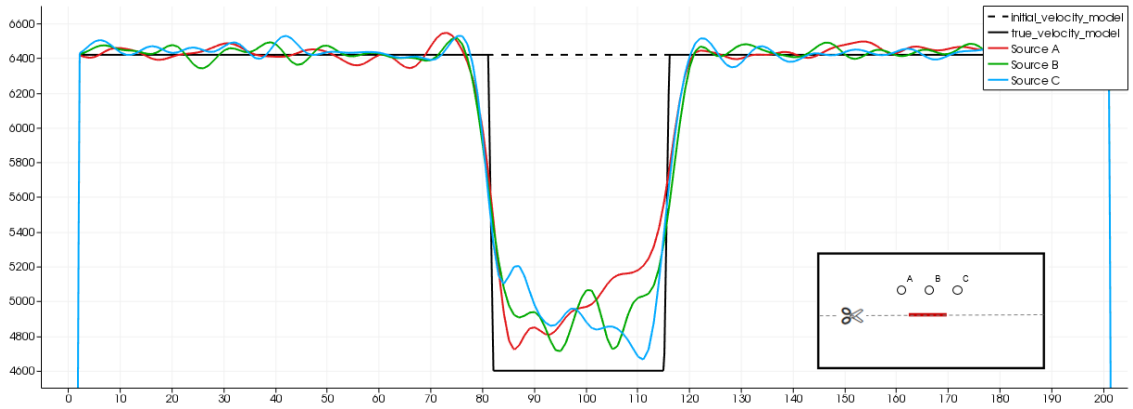

(a) Cut through crack for complete wavefield

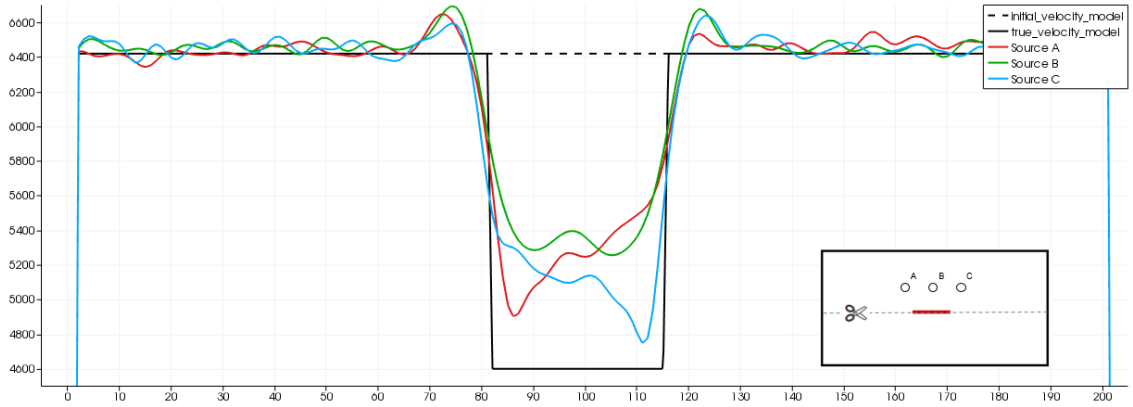

(b) Cut through Crack for known boudary

Figure 7. Quality of final velocity models for different source placements for the horizontal crack example in the cases of: a complete information and b boundary information.

approach to reduce this dependence is to perform multiple experiments with varying source position. If a sequence of experiments is performed with K different source positions, it will lead to a generalized misfit functional.

$$\chi(m) = \frac{1}{2}\sum_{k=1}^{K}\sum_{i=1}^{N}\int_0^T\int_\Omega [u(m,s_k;x,t) - u^0(s_k;x,t)]^2\delta(x-x_i^r)\,\mathrm{d}t\,\mathrm{d}x \tag{20}$$

In the next computation, the setup is the same as before but three experiments are combined in a larger minimization where the source position is varied from position A over position B to position C. To inspect the quality of the inversion, the cut through the crack is used again. Figure 8b shows the results in this scenario. The wave speeds are clearly closer to the true wave speeds and all choices of sensors provide sufficient information on crack position, dimension and orientation, even in the case of only four sensors. Especially the dimension of the crack is recovered well in all computations. In the case of complete boundary measurements even the wave speed in the crack is captured correctly. This shows that the inversion results can be improved by adding new experiments even when only few sensors are available. Nevertheless, the accuracy is still decreased and the noise outside of the crack is increased using less sensors.

To inspect the influence of additional sources, the next experiment is set up like the previous one but six additional sources are added. Again, all four boundary cases are considered. The setup and inversion results are shown in Figure 8c. For sixteen and ten sensors, the crack is almost

Figure 8. Final velocity models for different source and sensor placements for the horizontal crack example in the case of few available sensors. From top to bottom the number of experiments is increased. The setup of sources and sensors is shown on the right. In the case of ten sensors only the sensors depicted by green diamonds and the two red sensors on top and bottom were used. In the case of four sensors only the sensors depicted by red boxes are used.

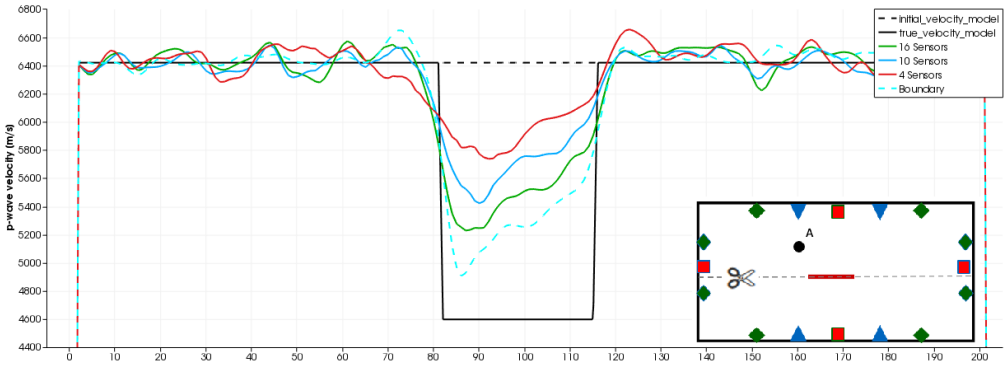

(a) Thin boundary - source A

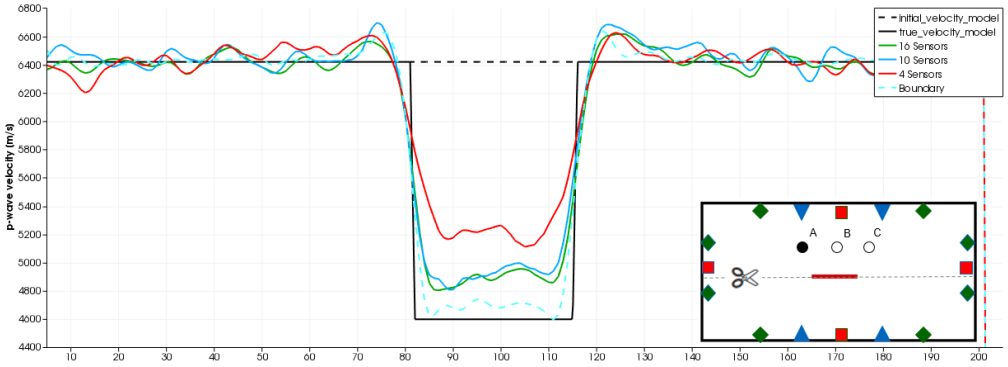

(b) Thin boundary - sources A,B and C

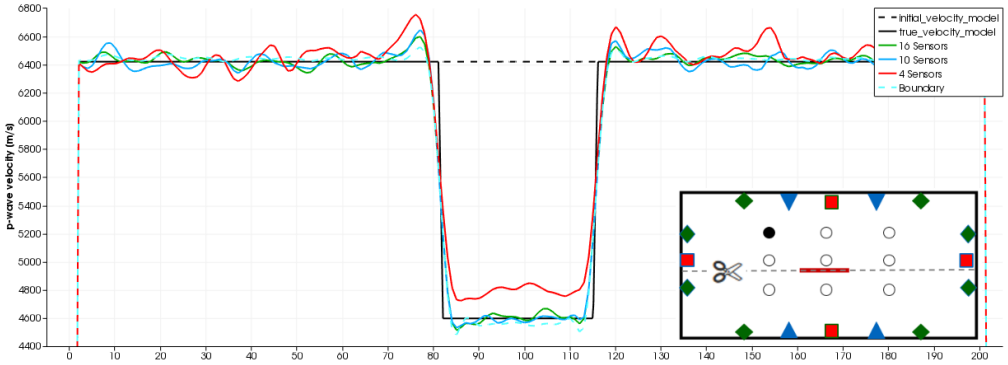

(c) Thin boundary - Nine Sources

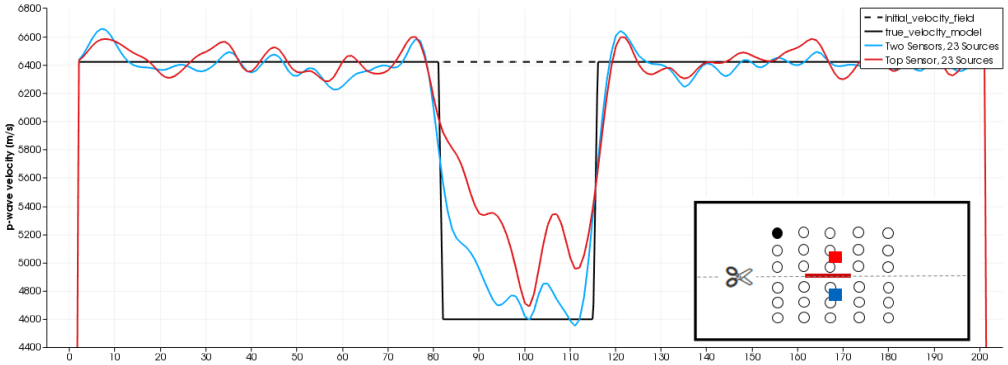

(d) Few sensors - 23 sources

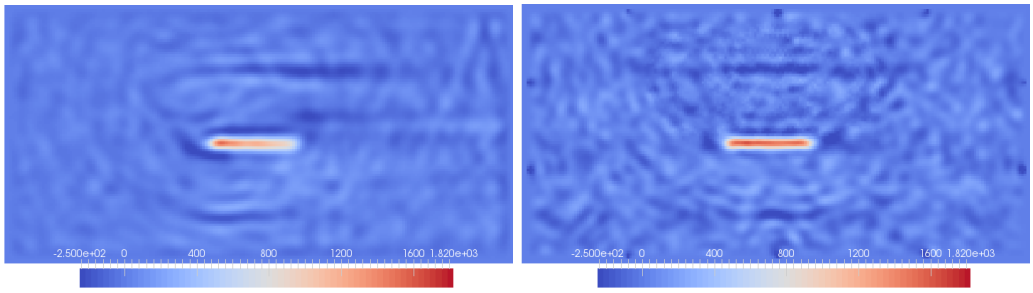

(a) Sensors on complete boundary and source at position A. See Figure 8a

(b) 10 Sensors on boundary and combined experiments with source at positions A, B and C. See Figure 8b

(c) Four sensors on boundary and nine combined experiments. See Figure 8c

(d) Two sensors close to crack and 25 combined experiments. See Figure 8d

Figure 9. Overall inversion results for different settings.

reconstructed perfectly. Also for only four sensors the true wave speed is accurately captured and the result still reveals all important details about crack location, dimension and orientation. Clearly, the combination of additional experiments leads to a steady increase in the accuracy of the inversion.

Prior knowledge and very sparse sensor measurements

The next computation incorporates prior information of the crack location. The setup is as before but only two and one sensors close to the crack are considered and 23 experiments are performed. The setup is shown on the right of Figure 8d. In the case of only one sensor the red one on the top is used. Because of prior knowledge of the crack location, the sources follow a path that is close to the unknown crack. The results of this extreme case are shown in Figure 8d. Even though only a minimum amount of sensors is used, still the results give a good impression on position, orientation and dimension of the unknown crack. Summarizing the results, Figure 9 shows the overall inversion results for some of the test cases.

5 Conclusion

A new NDT system based on an adaptive wave speed model has been presented. The method is based on the concept of full waveform inversion from seismology and extends it to the special case of US NDT by combining multiple experiments. It is able to detect position, dimension and orientation of a crack. This was shown for a simple numerical example of an aluminum plate. The quality of the detection depends on the amount and positioning of the sensors and the relative position of the source to the crack. In the realistic case of only very few available sensor measurements one single experiment is usually not enough to generate accurate results. Therefore, the general methodology was adapted to the NDT environment where the number of possible sensors is fixed to a small amount. By reformulating a misfit as combination of repeated experiments with changing source

location, it was possible to combine multiple experiments in one overall minimization. This proved to give significantly better results than in the single experiment case. Additionally, it should be mentioned that this method is not restricted to detect single cracks but, because of its very general setup, it can be used to detect multiple different cracks at once.
Algorithmically, going from simple steepest descent to conjugate gradient or higher order optimization schemes, a more efficient computation of the step length, and regularization should all result in a more efficient method.
In an important next step, it is planned to validate the results by coupling the simulation method with sensor data from real experiments.

References

Amitt, E., Givoli, D., and Turkel, E. (2014). Time reversal for crack identification. *Computational Mechanics*, 54(2):443–459. 00001.

Bletzinger, K.-U. and Ramm, E. (2014). Computational form finding and optimization. In *Shell Structures for Architecture: Form Finding and Optimization*, pages 45–56. Routledge. 00001.

Blitz, J. and Simpson, G. (1996). *Ultrasonic methods of non-destructive testing*. Non-destructive evaluation series. Chapman & Hall, London.

Chakroun, N., Fink, M., and Wu, F. (1992). Ultrasonic nondestructive testing with time reversal mirrors. pages 809–814. IEEE.

Drinkwater, B. W. and Wilcox, P. D. (2006). Ultrasonic arrays for non-destructive evaluation: A review. *NDT & E International*, 39(7):525–541.

Errico, R. M. (1997). What Is an Adjoint Model? *Bulletin of the American Meteorological Society*, 78(11):2577–2591.

Farova, Z. and Krus, V. (2012). Progressive Approaches to Localization and Identification of AE Sources. In *Proceedings of the 30th European Conference on Acoustic Emission Testing & 7th International Conference on Acoustic Emission*, pages 626–640, Granada. Universidad de Granada. 00000.

Fathi, A., Kallivokas, L. F., and Poursartip, B. (2015). Full-waveform inversion in three-dimensional PML-truncated elastic media. *Computer Methods in Applied Mechanics and Engineering*, 296:39–72.

Fichtner, A. (2011). *Full Seismic Waveform Modelling and Inversion*. Advances in Geophysical and Environmental Mechanics and Mathematics. Springer, Heidelberg.

Fink, M. (1997). Fink, M., "Time-reversal acoustics ," Physics Today, Vol. 50, No. 3, 34-40. *Physics Today*, 50(3):34–40. 00000.

Fink, M., Cassereau, D., Derode, A., Prada, C., Roux, P., Tanter, M., Thomas, J.-L., and Wu, F. (2000). Time-reversed acoustics. *Reports on Progress in Physics*, 63(12):1933–1995. 00631.

Fletcher, R. (2008). *Practical methods of optimization*. Wiley, Chichester.

Gauger, N. R. (2002). Aerodynamic Shape Optimization. *J.Aero.Soc.of India*, 54(3):246–254.

Giles, M. B. and Pierce, N. A. (1997). Adjoint equations in CFD: duality, boundary conditions and solution behaviour. *AIAA*, 97:1850.

Giles, M. B. and Pierce, N. A. (2000). An introduction to the adjoint approach to design. *Flow, turbulence and combustion*, 65(3-4):393–415. 00444.

Givoli, D. and Turkel, E. (2012). Time reversal with partial information for wave refocusing and scatterer identification. *Computer Methods in Applied Mechanics and Engineering*, 213-216:223–242. 00006.

Grosse, C. U. (2008). *Acoustic emission testing: basics for research - applications in civil engineering*. Springer, New York. 00000.

Jameson, A. (1988). Aerodynamic design via control theory. *Journal of scientific computing*, 3(3):233–260. 01107.

Kremers, S., Fichtner, A., Brietzke, G. B., Igel, H., Larmat, C., Huang, L., and Kser, M. (2011). Exploring the potentials and limitations of the time-reversal imaging of finite seismic sources. *Solid Earth*, 2(1):95–105. 00010.

Larmat, C. S., Guyer, R. A., and Johnson, P. A. (2010). Time-reversal methods in geophysics. *Phys. Today*, 63(8):31–35. 00031.

LeVeque, R. J. (2007). *Finite difference methods for ordinary and partial differential equations: steady-state and time-dependent problems*. Society for Industrial and Applied Mathematics, Philadelphia, PA.

Lions, J.-L. (1971). *Optimal control of systems governed by partial differential equations*. Springer-Verlag, Berlin; New York. 03502.

Marchuk, G. I. (1995). *Adjoint Equations and Analysis of Complex Systems*. Springer, Dordrecht.

Newman III, J. C., Taylor III, A. C., Barnwell, R. W., Newman, P. A., and Hou, G. J.-W. (1999). Overview of Sensitivity Analysis and Shape Optimization for Complex Aerodynamic Configurations. *Journal of Aircraft*, 36(1):87–96. 00116.

Nocedal, J. and Wright, S. J. (1999). *Numerical optimization*. Springer series in operations research. Springer, New York.

Polak, E. (1997). *Optimization: algorithms and consistent approximations*. Number 124 in Applied mathematical sciences. Springer, New York.

Quarteroni, A., Sacco, R., and Saleri, F. (2000). *Numerical mathematics*. Number 37 in Texts in applied mathematics. Springer, New York.

Tromp, J., Komattisch, D., and Liu, Q. (2008). Spectral-element and adjoint methods in seismology. *Communications in Computational Physics*, 3(1):1–32. 00133.